
Data-adaptive probabilistic likelihood approximation for ordinary differential equations

Mohan Wu

Department of Statistics and Actuarial Science
 University of Waterloo
 mhwu@uwaterloo.ca

Martin Lysy

Department of Statistics and Actuarial Science
 mlysy@uwaterloo.ca

Abstract

Parameter inference for ordinary differential equations (ODEs) is of fundamental importance in many scientific applications. While ODE solutions are typically approximated by deterministic algorithms, new research on probabilistic solvers indicates that they produce more reliable parameter estimates by better accounting for numerical errors. However, many ODE systems are highly sensitive to their parameter values. This produces deep local minima in the likelihood function – a problem which existing probabilistic solvers have yet to resolve. Here, we show that a Bayesian filtering paradigm for probabilistic ODE solution can dramatically reduce sensitivity to parameters by learning from the noisy ODE observations in a data-adaptive manner. Our method is applicable to ODEs with partially unobserved components and with arbitrary non-Gaussian noise. Several examples demonstrate that it is more accurate than existing probabilistic ODE solvers, and even in some cases than the exact ODE likelihood.

1 Introduction

Parameter estimation for ordinary differential equations (ODEs) is an important machine learning problem in the natural sciences and engineering, which typically involves repeatedly solving the ODE at each evaluation of the likelihood function. However, many ODE systems are hypersensitive to their input parameters, resulting in sharp local maxima in the likelihood function from which parameter search algorithms may fail to escape [27, 9, 12, 34, 16].

Since most ODEs do not have-closed form solutions, they must be approximated by numerical methods. Traditionally this has been done with deterministic algorithms [e.g., 7, 21, 1]. However, a growing body of work in *probabilistic numerics* [13, 40, 22] indicates that probabilistic ODE solvers, which directly account for uncertainty in the numerical approximation, provide more reliable parameter estimates in ODE learning problems [10, 11]. In particular, probabilistic solvers have the ability to condition on the observed data to guide the ODE solution, which can decrease sensitivity to model parameters [10, 46, 36, 43]. However, due to the added complexity of probabilistic solvers relative to their deterministic counterparts, their potential to reduce parameter hypersensitivity in a computationally efficient manner has yet to be fully realized.

Here we present a novel Data-Adaptive probabiLisTic ODE likelihQod approximatioN (DALTON) which attempts to bridge this gap. At the heart of our approach is a Bayesian filtering paradigm [42] particularly noted for its high accuracy and linear complexity in both time discretization points and

the number of system variables [e.g., 29, 4, 5, 43]. We show how to approximately condition on the observed data in the forward pass of this Bayesian filtering model, allowing for data which is both partially unobserved and subject to arbitrary non-Gaussian measurement errors. Several examples illustrate that DALTON is more accurate than leading probabilistic ODE parameter learning methods, and in the extreme case of chaotic ODE systems, is more reliable even than using the true ODE likelihood itself.

2 Background

DALTON is designed to solve arbitrary-order multi-variable ODE systems which satisfy an initial value problem (IVP). For a multi-variable function $\mathbf{x}(t) = (x_1(t), \dots, x_d(t))$, an ODE-IVP is of the form

$$\mathbf{W}\mathbf{X}(t) = \mathbf{f}(\mathbf{X}(t), t), \quad \mathbf{X}(0) = \mathbf{v}, \quad t \in [0, T], \quad (1)$$

where $\mathbf{X}(t) = (\mathbf{X}_1(t), \dots, \mathbf{X}_d(t))$, $\mathbf{X}_k(t) = (x_k^{(0)}(t), \dots, x_k^{(q_k-1)}(t))$ contains $x_k(t) = x_k^{(0)}(t)$ and its first $q_k - 1$ derivatives, $\mathbf{W} = (\mathbf{W}_1, \dots, \mathbf{W}_d)$ are coefficient matrices with $\mathbf{W}_k \in \mathbb{R}^{r_k \times q_k}$ and $\mathbf{f} = (\mathbf{f}_1, \dots, \mathbf{f}_d)$ are nonlinear functions with \mathbf{f}_k representing r_k equations for $k = 1, \dots, d$. For the usual ODE-IVP formulation of $\frac{d}{dt}\mathbf{X}(t) = \mathbf{f}(\mathbf{X}(t), t)$, we have $\mathbf{W}_k = [\mathbf{0}_{(q_k-1) \times 1} \mid \mathbf{I}_{(q_k-1) \times (q_k-1)}]$ for $k = 1, \dots, d$.

Unlike deterministic solvers, DALTON employs a probabilistic approach to solving (1) based on a well-established paradigm of Bayesian nonlinear filtering [42, 36, 43]. This approach consists of putting a Gaussian Markov process prior on $\mathbf{X}(t)$, and updating it with information from the ODE-IVP (1) at time points $t = t_0, \dots, t_N$, where $t_n = n \cdot \Delta t$, $\Delta t = T/N$. Specifically, let $\mathbf{X}_n = \mathbf{X}(t_n)$ and consider the general indexing notation $\mathbf{X}_{m:n} = (\mathbf{X}_m, \dots, \mathbf{X}_n)$. If $\mathbf{X}(t)$ is the solution to (1), we would have $\mathbf{Z}_n = \mathbf{W}\mathbf{X}_n - \mathbf{f}(\mathbf{X}_n, t_n) = \mathbf{0}$. Based on this observation, [42] consider a state-space model in \mathbf{X}_n and \mathbf{Z}_n of the form

$$\begin{aligned} \mathbf{X}_{n+1} \mid \mathbf{X}_n &\sim \mathcal{N}(\mathbf{Q}\mathbf{X}_n, \mathbf{R}) \\ \mathbf{Z}_n &\stackrel{\text{ind}}{\sim} \mathcal{N}(\mathbf{W}\mathbf{X}_n - \mathbf{f}(\mathbf{X}_n, t_n), \mathbf{V}_n), \end{aligned} \quad (2)$$

where $\mathbf{X}_0 = \mathbf{v}$, $\mathbf{Q} = \mathbf{Q}(\Delta t)$ and $\mathbf{R} = \mathbf{R}(\Delta t)$ are determined by the Gaussian Markov process prior, and \mathbf{V}_n is a tuning parameter. The specific Gaussian Markov process prior used in this work is described in Appendix A. The stochastic ODE solution is then given by the posterior distribution $p(\mathbf{X}_{0:N} \mid \mathbf{Z}_{0:N} = \mathbf{0})$ resulting from model (2).

As $N \rightarrow \infty$ and $\mathbf{V}_n \rightarrow \mathbf{0}$, the posterior distribution $p(\mathbf{X}_{0:N} \mid \mathbf{Z}_{0:N} = \mathbf{0})$ gets arbitrarily close to the true ODE solution. However, this posterior distribution generally cannot be sampled from directly. Alternatives include Markov chain Monte Carlo sampling [46] and particle filtering [42]. A less accurate but ostensibly much faster approach is to linearize (2), resulting in the working model

$$\begin{aligned} \mathbf{X}_{n+1} \mid \mathbf{X}_n &\sim \mathcal{N}(\mathbf{Q}\mathbf{X}_n, \mathbf{R}) \\ \mathbf{Z}_n &\stackrel{\text{ind}}{\sim} \mathcal{N}((\mathbf{W} + \mathbf{B}_n)\mathbf{X}_n + \mathbf{a}_n, \mathbf{V}_n), \end{aligned} \quad (3)$$

The benefit of the linearized model (3) is that it gives an approximation to the posterior distribution $p(\mathbf{X}_{0:N} \mid \mathbf{Z}_{0:N} = \mathbf{0})$ – and the marginal likelihood $p(\mathbf{Z}_{0:N})$, which we will need in Section 3 – having linear complexity $\mathcal{O}(N)$ in the number of time discretization points, using standard Kalman filtering and smoothing techniques [42, 38]. Many linearization approaches can be found in [42, 29]. Perhaps one of the simplest [38] has $\mathbf{V}_n = \mathbf{0}$ and uses a zeroth order Taylor approximation for the nonlinear ODE function,

$$\mathbf{f}(\mathbf{X}_n, t_n) \approx \mathbf{f}(\boldsymbol{\mu}_{n|n-1}, t_n), \quad (4)$$

where $\boldsymbol{\mu}_{n|n-1} = E[\mathbf{X}_n \mid \mathbf{Z}_{0:n-1}]$ is the predicted mean obtained sequentially from a Kalman filter applied to (3), i.e., with $\mathbf{a}_n = -\mathbf{f}(\boldsymbol{\mu}_{n|n-1}, t_n)$ and $\mathbf{B}_n = \mathbf{0}$.

3 Methodology

The parameter-dependent extension of the ODE-IVP (1) is of the form

$$\mathbf{W}_\theta \mathbf{X}(t) = \mathbf{f}(\mathbf{X}(t), t, \theta), \quad \mathbf{X}(0) = \mathbf{v}_\theta, \quad t \in [0, T]. \quad (5)$$

The learning problem consists of estimating the unknown parameters θ which determine $\mathbf{X}(t)$ in (5) from noisy observations $\mathbf{Y}_{0:M} = (\mathbf{Y}_0, \dots, \mathbf{Y}_M)$, recorded at times $t = t'_0, \dots, t'_M$ under the measurement model

$$\mathbf{Y}_i \stackrel{\text{ind}}{\sim} p(\mathbf{Y}_i \mid \mathbf{X}(t'_i), \phi). \quad (6)$$

In terms of the ODE solver discretization time points $t = t_0, \dots, t_N$, $N \geq M$, consider the mapping $n(\cdot)$ such that $t_{n(i)} = t'_i$. DALTON then augments the Bayesian filtering model (2) to account for noisy observations from (6) via

$$\begin{aligned} \mathbf{X}_{n+1} \mid \mathbf{X}_n &\sim \mathcal{N}(\mathbf{Q}_\eta \mathbf{X}_n, \mathbf{R}_\eta) \\ \mathbf{Z}_n &\stackrel{\text{ind}}{\sim} \mathcal{N}(\mathbf{W} \mathbf{X}_n - \mathbf{f}(\mathbf{X}_n, t_n, \theta), \mathbf{V}_n) \\ \mathbf{Y}_i &\stackrel{\text{ind}}{\sim} p(\mathbf{Y}_i \mid \mathbf{X}_{n(i)}, \phi), \end{aligned} \quad (7)$$

where the Gaussian Markov process parameters \mathbf{Q}_η and \mathbf{R}_η depend on tuning parameters η . The likelihood function induced by the probabilistic solver corresponding to (7) for all parameters $\Theta = (\theta, \phi, \eta)$ is given by

$$p(\mathbf{Y}_{0:M} \mid \mathbf{Z}_{0:N} = \mathbf{0}, \Theta). \quad (8)$$

3.1 Gaussian Measurement Model

First suppose the observations of (6) consist of Gaussian noise,

$$\mathbf{Y}_i \stackrel{\text{ind}}{\sim} \mathcal{N}(\mathbf{D}_i^\phi \mathbf{X}_{n(i)}, \Omega_\phi), \quad (9)$$

where \mathbf{D}_i^ϕ is a (possibly ϕ -dependent) coefficient matrix. To compute the likelihood (8), we begin with the identity

$$p(\mathbf{Y}_{0:M} \mid \mathbf{Z}_{0:N} = \mathbf{0}, \Theta) = \frac{p(\mathbf{Y}_{0:M}, \mathbf{Z}_{0:N} = \mathbf{0} \mid \Theta)}{p(\mathbf{Z}_{0:N} = \mathbf{0} \mid \Theta)}. \quad (10)$$

The denominator $p(\mathbf{Z}_{0:N} = \mathbf{0} \mid \Theta)$ on the right-hand side can be computed using a Kalman filter on the data-free linearization described in Section 2 [e.g., 42, 38, and see details in Algorithm 1]. In fact, the same can be done for the numerator $p(\mathbf{Y}_{0:M}, \mathbf{Z}_{0:N} = \mathbf{0} \mid \Theta)$ by linearizing as follows:

- At time points $t_n \notin \{t_{n(0)}, \dots, t_{n(M)}\}$ where no observations are recorded, apply the data-free linearization (3).
- At the time points $t_n = t_{n(i)}$ where the observations are recorded, since the augmented measurement variables $\mathbf{Z}_{n(i)}$ and \mathbf{Y}_i are conditionally independent given $\mathbf{X}_{n(i)}$, linearize them jointly via

$$\begin{bmatrix} \mathbf{Z}_{n(i)} \\ \mathbf{Y}_i \end{bmatrix} \stackrel{\text{ind}}{\sim} \mathcal{N} \left(\left(\begin{bmatrix} \mathbf{W}_\theta \\ \mathbf{D}_i^\phi \end{bmatrix} + \begin{bmatrix} \mathbf{B}_{n(i)} \\ \mathbf{0} \end{bmatrix} \right) \mathbf{X}_{n(i)} - \begin{bmatrix} \mathbf{a}_{n(i)} \\ \mathbf{0} \end{bmatrix}, \begin{bmatrix} \mathbf{V}_{n(i)} & \mathbf{0} \\ \mathbf{0} & \Omega_\phi \end{bmatrix} \right), \quad (11)$$

where the data-free linearization coefficients $\mathbf{a}_{n(i)}$, $\mathbf{B}_{n(i)}$, and $\mathbf{V}_{n(i)}$ are computed exactly as in (3).

In other words, DALTON uses both \mathbf{Y}_i and $\mathbf{Z}_{n(i)}$ to update the Kalman filter when data is observed and only \mathbf{Z}_n when it is not. The complete algorithm is provided in Algorithm 1, in terms of the standard Kalman filtering and smoothing recursions detailed in Appendix B.

3.2 Non-Gaussian Measurement Model

Let us now turn to the general measurement model (6), which we write as

$$\mathbf{Y}_i \stackrel{\text{ind}}{\sim} \exp\{-g_i(\mathbf{Y}_i \mid \mathbf{x}_{n(i)}, \phi)\}, \quad (12)$$

where $\mathbf{x}_{n(i)}$ is the subset of $\mathbf{X}_{n(i)}$ corresponding to the partially observed components of $\mathbf{X}(t)$, which may depend on the time point $t = t_{n(i)}$.

In order to compute the likelihood (8), we consider a different identity,

$$\begin{aligned} p(\mathbf{Y}_{0:M} \mid \mathbf{Z}_{0:N} = \mathbf{0}, \Theta) &= \frac{p(\mathbf{Y}_{0:M}, \mathbf{X}_{0:N} \mid \mathbf{Z}_{0:N} = \mathbf{0}, \Theta)}{p(\mathbf{X}_{0:N} \mid \mathbf{Y}_{0:M}, \mathbf{Z}_{0:N} = \mathbf{0}, \Theta)} \\ &= \frac{p(\mathbf{X}_{0:N} \mid \mathbf{Z}_{0:N} = \mathbf{0}, \theta, \eta) \times \prod_{i=0}^M \exp\{-g_i(\mathbf{Y}_i \mid \mathbf{x}_{n(i)}, \phi)\}}{p(\mathbf{X}_{0:N} \mid \mathbf{Y}_{0:M}, \mathbf{Z}_{0:N} = \mathbf{0}, \Theta)}, \end{aligned} \quad (13)$$

Algorithm 1 DALTON probabilistic ODE likelihood approximation for Gaussian measurements.

```

1: procedure DALTON( $\mathbf{W}_\theta, \mathbf{f}(\mathbf{X}, t, \theta), \mathbf{v}_\theta, \mathbf{Q}_\eta, \mathbf{R}_\eta, \mathbf{Y}_{0:M}, \mathbf{D}_{0:M}^\phi, \boldsymbol{\Omega}_\phi$ )
2:    $\mu_{0|0}, \Sigma_{0|0} \leftarrow \mathbf{v}, \mathbf{0}$                                  $\triangleright$  Initialization
3:    $\mathbf{Z}_{0:N} \leftarrow \mathbf{0}$ 
4:    $\ell_z, \ell_{yz} \leftarrow 0, 0$ 
5:    $i \leftarrow 0$                                  $\triangleright$  Used to map  $t_n$  to  $t_i'$ 
6:    $\triangleright$  Lines 7-12 compute  $\log p(\mathbf{Z}_{0:N} = \mathbf{0} \mid \boldsymbol{\Theta})$ 
7:   for  $n = 0 : N$  do
8:      $\mu_{n|n-1}, \Sigma_{n|n-1} \leftarrow \text{kalman\_predict}(\mu_{n-1|n-1}, \Sigma_{n-1|n-1}, \mathbf{0}, \mathbf{Q}_\eta, \mathbf{R}_\eta)$ 
9:      $\mathbf{a}_n, \mathbf{B}_n, \mathbf{V}_n \leftarrow \text{linearize}(\mu_{n|n-1}, \Sigma_{n|n-1}, \mathbf{W}_\theta, \mathbf{f}(\mathbf{X}, t_n, \theta))$ 
10:     $\mu_n, \Sigma_n \leftarrow \text{kalman\_forecast}(\mu_{n|n-1}, \Sigma_{n|n-1}, \mathbf{W}_\theta, \mathbf{a}_n, \mathbf{B}_n, \mathbf{V}_n)$ 
11:     $\ell_z \leftarrow \ell_z + \text{normal\_logpdf}(\mathbf{Z}_n = \mathbf{0}; \mu_n, \Sigma_n)$ 
12:     $\mu_{n|n}, \Sigma_{n|n} \leftarrow \text{kalman\_update}(\mu_{n|n-1}, \Sigma_{n|n-1}, \mathbf{W}_\theta, \mathbf{Z}_n, \mathbf{a}_n, \mathbf{B}_n, \mathbf{V}_n)$ 
13:     $\triangleright$  Lines 14-24 compute  $\log p(\mathbf{Y}_{0:M}, \mathbf{Z}_{0:N} = \mathbf{0} \mid \boldsymbol{\Theta})$ 
14:     $\ell_{yz} \leftarrow \text{normal\_logpdf}(\mathbf{Y}_0; \mathbf{D}_0^\phi \mathbf{v}_\theta, \Sigma_\phi)$ 
15:    for  $n = 0 : N$  do
16:       $\mu_{n|n-1}, \Sigma_{n|n-1} \leftarrow \text{kalman\_predict}(\mu_{n-1|n-1}, \Sigma_{n-1|n-1}, \mathbf{0}, \mathbf{Q}_\eta, \mathbf{R}_\eta)$ 
17:       $\mathbf{a}_n, \mathbf{B}_n, \mathbf{V}_n \leftarrow \text{linearize}(\mu_{n|n-1}, \Sigma_{n|n-1}, \mathbf{W}_\theta, \mathbf{f}(\mathbf{X}, t_n, \theta))$ 
18:      if  $t_n = t_{n(i)}$  then
19:         $\mathbf{Z}_n \leftarrow \begin{bmatrix} \mathbf{Z}_n \\ \mathbf{Y}_i \end{bmatrix}, \quad \mathbf{W}_\theta \leftarrow \begin{bmatrix} \mathbf{W}_\theta \\ \mathbf{D}_i^\phi \end{bmatrix}, \quad \mathbf{B}_n \leftarrow \begin{bmatrix} \mathbf{B}_n \\ \mathbf{0} \end{bmatrix}$ 
20:         $\mathbf{a}_n \leftarrow \begin{bmatrix} \mathbf{a}_n \\ \mathbf{0} \end{bmatrix}, \quad \mathbf{V}_n \leftarrow \begin{bmatrix} \mathbf{V}_n & \mathbf{0} \\ \mathbf{0} & \boldsymbol{\Omega}_\phi \end{bmatrix}$ 
21:         $i \leftarrow i + 1$ 
22:       $\mu_n, \Sigma_n \leftarrow \text{kalman\_forecast}(\mu_{n|n-1}, \Sigma_{n|n-1}, \mathbf{W}_\theta, \mathbf{a}_n, \mathbf{B}_n, \mathbf{V}_n)$ 
23:       $\ell_{yz} \leftarrow \ell_{yz} + \text{normal\_logpdf}(\mathbf{Z}_n; \mu_n, \Sigma_n)$ 
24:       $\mu_{n|n}, \Sigma_{n|n} \leftarrow \text{kalman\_update}(\mu_{n|n-1}, \Sigma_{n|n-1}, \mathbf{W}_\theta, \mathbf{Z}_n, \mathbf{a}_n, \mathbf{B}_n, \mathbf{V}_n)$ 
25:
26:   return  $\ell_{yz} - \ell_z$                                  $\triangleright$  Estimate of  $\log p(\mathbf{Y}_{0:M} \mid \mathbf{Z}_{0:N} = \mathbf{0}, \boldsymbol{\Theta})$ 

```

where the identity holds for any value of $\mathbf{X}_{0:N}$. In the numerator of (13), $p(\mathbf{X}_{0:N} \mid \mathbf{Z}_{0:N} = \mathbf{0}, \boldsymbol{\Theta})$ can be approximated using the Kalman smoothing algorithm applied to the data-free linearization (3), whereas the product term is obtained via straightforward calculation of (12). As for the denominator of (13), we propose to approximate it by a multivariate normal distribution as follows. First, we note that

$$\log p(\mathbf{X}_{0:N} \mid \mathbf{Y}_{0:M}, \mathbf{Z}_{0:N} = \mathbf{0}, \boldsymbol{\Theta}) = \log p(\mathbf{X}_{0:N} \mid \mathbf{Z}_{0:N} = \mathbf{0}, \theta, \eta) - \sum_{i=0}^M g_i(\mathbf{Y}_i \mid \mathbf{x}_{n(i)}, \phi) + c_1, \quad (14)$$

where c_1 is constant with respect to $\mathbf{X}_{0:N}$. Next, we take a second-order Taylor expansion of $h_i(\mathbf{x}_{n(i)}) = g_i(\mathbf{Y}_i \mid \mathbf{x}_{n(i)}, \phi)$ about $\mathbf{x}_{n(i)} = \hat{\mathbf{x}}_{n(i)}$. After simplification this gives

$$h_i(\mathbf{x}_{n(i)}) \approx -\frac{1}{2}(\mathbf{x}_{n(i)} - \hat{\mathbf{Y}}_i)' \nabla^2 h_i(\hat{\mathbf{x}}_{n(i)})(\mathbf{x}_{n(i)} - \hat{\mathbf{Y}}_i) + c_2, \quad (15)$$

where ∇h_i and $\nabla^2 h_i$ are the gradient and hessian of h_i , $\hat{\mathbf{Y}}_i = \hat{\mathbf{x}}_{n(i)} - \nabla^2 h_i(\hat{\mathbf{x}}_{n(i)})^{-1} \nabla h_i(\hat{\mathbf{x}}_{n(i)})$, and c_2 is constant with respect to $\mathbf{x}_{n(i)}$. Substituting the quadratic approximation (15) into (14), and using the data-free linearization of $p(\mathbf{X}_{0:N} \mid \mathbf{Z}_{0:N} = \mathbf{0}, \theta, \eta)$, we may estimate $p(\mathbf{X}_{0:N} \mid \mathbf{Y}_{0:M}, \mathbf{Z}_{0:N} = \mathbf{0}, \boldsymbol{\Theta})$ as the multivariate normal arising from the working model

$$\begin{aligned} \mathbf{X}_{n+1} \mid \mathbf{X}_n &\sim \mathcal{N}(\mathbf{Q}_\eta \mathbf{X}_n, \mathbf{R}_\eta) \\ \mathbf{Z}_n &\stackrel{\text{ind}}{\sim} \mathcal{N}((\mathbf{W}_\theta + \mathbf{B}_n) \mathbf{X}_n + \mathbf{a}_n, \mathbf{V}_n) \\ \hat{\mathbf{Y}}_i &\stackrel{\text{ind}}{\sim} \mathcal{N}(\mathbf{x}_{n(i)}, [\nabla^2 h_i(\hat{\mathbf{x}}_{n(i)})]^{-1}), \end{aligned} \quad (16)$$

where the data-free linearization coefficients $\mathbf{a}_{n(i)}$, $\mathbf{B}_{n(i)}$, and $\mathbf{V}_{n(i)}$ are computed exactly as in (3). Calculation of $p(\mathbf{X}_{0:N} \mid \mathbf{Y}_{0:M}, \mathbf{Z}_{0:N} = \mathbf{0}, \boldsymbol{\Theta})$ the combines the Kalman forward pass of Algorithm (1) with the backward pass of a standard Kalman smoother. We are now left with the choice of

$\mathbf{X}_{0:N}$ to plug into (13) and the choice of $\hat{\mathbf{x}}_{n(i)}$ about which to perform the Taylor expansion (15). For the latter, we use $\hat{\mathbf{x}}_{n(i)} = E[\mathbf{x}_{n(i)} \mid \mathbf{Z}_{0:n(i)-1}, \hat{\mathbf{Y}}_{0:i-1}]$, the predicted mean obtained sequentially from the Kalman filter applied to (16). For the former, we use $\mathbf{X}_{0:N} = E[\mathbf{X}_{0:N} \mid \mathbf{Z}_{0:N} = \mathbf{0}, \hat{\mathbf{Y}}_{0:M}]$, the conditional mean of $\mathbf{X}_{0:N}$ given all the observed data in the working model (16), which is readily obtained from the Kalman filtering and smoothing recursions. Full details are provided in Algorithm 2 in Appendix C.

3.3 Heuristic Justification

We give a brief heuristic justification for the convergence of the DALTON approximation with arbitrary noise (13)-(16) to the true likelihood as $N \rightarrow \infty$ with $\mathbf{V}_n = \mathbf{0}$. First, it has been proved by [25] that $p(\mathbf{X}_{0:N} \mid \mathbf{Z}_{0:N}, \boldsymbol{\theta}, \boldsymbol{\eta})$ concentrates on the true ODE solution under the linearization (4). We assume that the same holds true for $p(\mathbf{X}_{0:N} \mid \mathbf{Y}_{0:M}, \mathbf{Z}_{0:N} = \mathbf{0}, \boldsymbol{\Theta})$ under the extended linearization of (16). Short of a formal proof, an informal justification is that $\mathbf{Y}_{0:M}$ adds only a finite amount of information to the posterior on $\mathbf{X}_{0:N}$, whereas $\mathbf{Z}_{0:N}$ adds an infinite amount as $N \rightarrow \infty$, thus ultimately overwhelming the information provided by the observed data. Since these two posteriors converge to the same value, we expect them to cancel out in (13), leaving just $\prod_{i=0}^M \exp\{-g_i(\mathbf{Y}_i \mid \mathbf{x}_{n(i)}, \boldsymbol{\phi})\}$ in the numerator of (13) with $\mathbf{X}_{0:N}$ the true ODE solution, which is precisely the form the true ODE likelihood.

4 Related Work

Various probabilistic ODE solvers have been presented in the works of e.g., [8, 14, 2, 37, 10, 23, 41, 11, 18, 20, 30, 42, 38, 45, 28, 24, 46, 44, 29, 4, 43, 5]. The Bayesian filtering paradigm (2) at the heart of many of these solvers was formulated in [42], alternatively viewed as a predictor-corrector method in [10, 38]. Various convergence properties of the corresponding probabilistic solver are derived in [10, 38, 25]. Within the Bayesian filtering framework, we highlight three approaches in which the ODE solver directly conditions on the observed data:

MAGI [46] estimates $\boldsymbol{\Theta}$ in a Bayesian context from the exact posterior $p(\boldsymbol{\Theta} \mid \mathbf{Y}_{0:M}, \mathbf{Z}_{0:N} = \mathbf{0})$ resulting from (7) with $\mathbf{V}_n = \mathbf{0}$. A similar approach is taken by [10] in the predictor-corrector formulation. Both methods require Markov chain Monte Carlo (MCMC) techniques to sample from the desired posterior, which requires at least an order of magnitude times more evaluations of the probabilistic ODE solver than the approximate Bayesian method based on DALTON we present in Section 5.

ProbNum [36] uses an extended Kalman filter similar to ours, but focuses on estimating the ODE solution itself rather than the model parameters.

Fenrir [43] extends an approach developed in [24]. It is fast, accurate, and compares favorably to state-of-the-art probabilistic and deterministic ODE solvers alike [43]. Fenrir begins by using the data-free linearization of (3) to estimate $p(\mathbf{X}_{0:N} \mid \mathbf{Z}_{0:N} = \mathbf{0}, \boldsymbol{\theta}, \boldsymbol{\eta})$. This model can be simulated from via a (non-homogeneous) Markov chain going backwards in time,

$$\begin{aligned} \mathbf{X}_N &\sim \mathcal{N}(\mathbf{b}_N, \mathbf{C}_N) \\ \mathbf{X}_n \mid \mathbf{X}_{n+1} &\sim \mathcal{N}(\mathbf{A}_n \mathbf{X}_n + \mathbf{b}_n, \mathbf{C}_n), \end{aligned} \tag{17}$$

where the coefficients $\mathbf{A}_{0:N-1}$, $\mathbf{b}_{0:N}$, and $\mathbf{C}_{0:N}$ can be derived using the Kalman filtering and smoothing recursions [43]. Next, Fenrir assumes that Gaussian observations are added to the model, from which

$$p(\mathbf{Y}_{0:M} \mid \mathbf{Z}_{0:N} = \mathbf{0}, \boldsymbol{\Theta}) = \int p(\mathbf{Y}_{0:N} \mid \mathbf{X}_{0:N}, \boldsymbol{\Theta}) p(\mathbf{X}_{0:N} \mid \mathbf{Z}_{0:N} = \mathbf{0}, \boldsymbol{\Theta}) d\mathbf{X}_{0:N} \tag{18}$$

is computed using a Kalman filter on the backward pass of (17). The key difference between DALTON and Fenrir is that the latter linearizes *before* adding the observations to the model (linearize-then-observe), whereas the former does so *after* (observe-then-linearize). Moreover, DALTON can be applied to non-Gaussian errors whereas Fenrir cannot.

5 Examples

We now examine the performance of DALTON in several numerical examples of parameter learning. We proceed with a Bayesian approach by postulating a prior distribution $\pi(\Theta)$ on the full set of parameters $\Theta = (\theta, \phi, \eta)$, which combined with (8) gives the DALTON posterior

$$p(\Theta | \mathbf{Y}_{0:M}) \propto \pi(\Theta) \times p(\mathbf{Y}_{0:M} | \mathbf{Z}_{0:N} = \mathbf{0}, \Theta). \quad (19)$$

Parameter inference is then accomplished by way of a Laplace approximation [e.g., 17], for which we have

$$\Theta | \mathbf{Y}_{0:M} \approx \mathcal{N}(\hat{\Theta}, \hat{V}_\Theta), \quad (20)$$

where $\hat{\Theta} = \arg \max_{\Theta} \log p(\Theta | \mathbf{Y}_{0:M})$ and $\hat{V}_\Theta = -[\frac{\partial^2}{\partial \Theta \partial \Theta} \log p(\Theta | \mathbf{Y}_{0:M})]^{-1}$. The Laplace approximation is a popular tool for Bayesian machine learning applications [32, 19], typically requiring at least an order of magnitude fewer evaluations of $p(\Theta | \mathbf{Y}_{0:M})$ than full Bayesian inference via MCMC. Our Python implementation of DALTON¹ uses the **JAX** library [6] for automatic differentiation and just-in-time (JIT) compilation. This produces very fast implementations of $\log p(\Theta | \mathbf{Y}_{0:M})$ and its gradient, by which we obtain $\hat{\Theta}$ using the Newton-CG optimization algorithm [33] as implemented in the **JAXopt** library [3].

In the examples below, we assume $\mathbf{X}(t) = \{\mathbf{X}_k(t) : k = 1, \dots, d\}$ has independent integrated Brownian motion (IBM) priors [38] of order $p = 3$ on each component $\mathbf{X}_k(t)$, which amounts to d prior process tuning parameters $\eta = (\sigma_1, \dots, \sigma_d)$ (details in Appendix A). Furthermore, for linearization we use the first-order Taylor approximation of [43], and use the blocking method of [29] to decrease computational complexity from $\mathcal{O}(N \cdot \{\sum_{k=1}^d q_k\}^3)$ to $\mathcal{O}(N \cdot \prod_{k=1}^d q_k^3)$ (details in Appendix D). We take the measurement model parameters ϕ to be known, such that the learning problem is only for the parameter η to tune the IBM prior, and the ODE model parameters $\theta = (\theta_1, \dots, \theta_D)$. We use a flat prior on η and independent $\mathcal{N}(0, 10^2)$ priors on either θ_r or $\log \theta_r$, $r = 1, \dots, D$, depending on whether θ_r is unbounded or $\theta_r > 0$. The Laplace approximation $p(\theta | \mathbf{Y}_{0:M}) \approx \mathcal{N}(\hat{\theta}, \hat{V}_\theta)$ was obtained from $(\hat{\theta}, \hat{\eta}) = \arg \max_{(\theta, \eta)} \log p(\Theta | \mathbf{Y}_{0:M})$ and $\hat{V}_\theta = -[\frac{\partial^2}{\partial \theta \partial \theta} \log p(\Theta | \mathbf{Y}_{0:M})]^{-1}$, i.e., with the hessian taken only with respect to θ and not η . This was found to produce slightly better results than when uncertainty is propagated through the prior process tuning parameters as well.

The experimental data are simulated using a very high accuracy deterministic solver for the ODE-IVP (5); namely, the Runge-Kutta 8 solver with Dormand-Prince step size adaptation [15] as implemented in the **diffraex** library [26]. We compare the parameter inference results of DALTON to those of a Laplace approximation with Fenrir, and with the **diffraex** deterministic ODE solver, which we refer to as RK. We shall assume that the output of RK is the true ODE solution.

5.1 FitzHugh-Nagumo Model

The FitzHugh-Nagumo (FN) model [39] is a two-state ODE on $\mathbf{x}(t) = (V(t), R(t))$, in which $V(t)$ describes the evolution of the neuronal membrane voltage and $R(t)$ describes the activation and deactivation of neuronal channels. The FN ODE is given by

$$\frac{dV(t)}{dt} = c \left(V(t) - \frac{V(t)^3}{3} + R(t) \right), \quad \frac{dR(t)}{dt} = -\frac{V(t) - a + bR(t)}{c}. \quad (21)$$

The model parameters are $\theta = (a, b, c, V(0), R(0))$, with $a, b, c > 0$, which are to be learned from the measurement model

$$\mathbf{Y}_i \stackrel{\text{ind}}{\sim} \mathcal{N}(\mathbf{x}(t_i), \phi^2 \cdot \mathbf{I}_{2 \times 2}), \quad (22)$$

where $t_i = i$ with $i = 0, 1, \dots, 40$ and $\phi^2 = 0.005$. The ODE and noisy observations are displayed in Figure 1(a).

Figure 1(b) displays the Laplace posteriors for DALTON and Fenrir for data simulated with true parameter values $\theta = (0.2, 0.2, 3, -1, 1)$, at different values of the solver step size $\Delta t = T/N$. Also included for comparison is the Laplace posterior for the true likelihood obtained with RK. At the largest step size $\Delta t = 0.25$, DALTON and Fenrir posteriors are similar with the notable

¹<https://github.com/mlsys/rodeo>

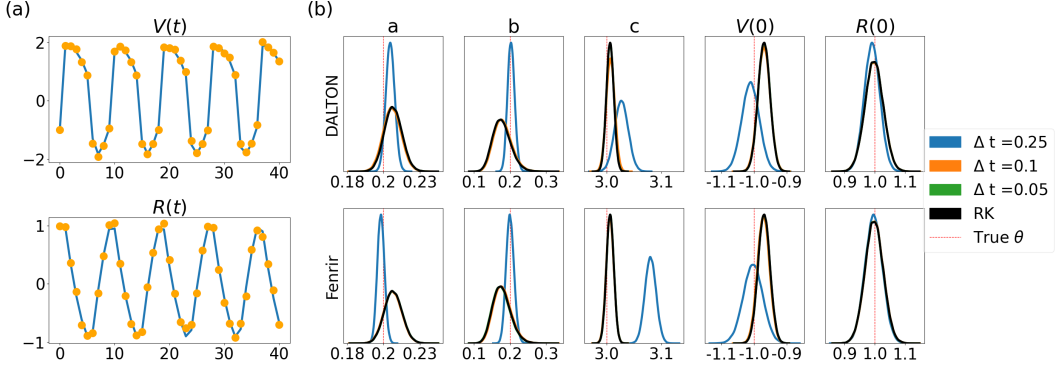


Figure 1: (a) ODE and noisy observations for the FN model. (b) Parameter posteriors for the FN model using various ODE solvers.

exception of the posterior for c , in which DALTON covers the true parameter value but Fenrir does not. This is because c controls the period of the quasi-oscillatory behavior of the FN model exhibited in Figure 1(a) [e.g., 35], which is a prime example of when incorporating information from the observed data on the forward pass (DALTON) rather than the backward pass (Fenrir) is most useful. At smaller step sizes, both DALTON and Fenrir converge to the true Laplace posterior. In terms of timing, the two probabilistic solvers are roughly the same, with Fenrir doing one forward and one backward pass on $t_{0:N}$, and DALTON doing one forward pass for each of $p(\mathbf{Z}_{0:N} = \mathbf{0} \mid \Theta)$ and $p(\mathbf{Y}_{0:M}, \mathbf{Z}_{0:N} = \mathbf{0} \mid \Theta)$ in (10).

5.2 FN Model with Non-Gaussian Noise

Using the same θ and t_i as in Section 5.1, we now suppose that the noisy observation model is

$$Y_{ij} \stackrel{\text{ind}}{\sim} \text{Poisson}(\exp\{b_0 + b_1 x_j(t_i)\}), \quad (23)$$

where $b_0 = 0.1$ and $b_1 = 0.5$. For comparison, we use a naive normal approximation to (23) with mean given by the first order Taylor approximation to $g(x_j(t_i)) = \exp\{b_0 + b_1 x_j(t_i)\}$ about the filtered mean $\mu_{ij} = E[x_j(t_i) \mid \mathbf{Z}_{0:n(i)-1}, \mathbf{Y}_{0:i-1}]$, and variance given by the zeroth order Taylor approximation to $g(x_j(t_i))$ about μ_{ij} . Then, we use this approximate measurement model in the Gaussian version of DALTON given in Algorithm 1. Figure 2 displays the parameter posteriors of this naive approximation along with the non-Gaussian DALTON approximation of Algorithm 2. The naive Gaussian DALTON is about twice as fast as non-Gaussian DALTON, since the former computes only two forward passes of the Kalman filter, whereas the latter requires forward and backward passes to compute the two forward and backward passes for each of $p(\mathbf{X}_{0:N} \mid \mathbf{Z}_{0:N} = \mathbf{0}, \theta, \eta)$ and $p(\mathbf{X}_{0:N} \mid \mathbf{Y}_{0:M}, \mathbf{Z}_{0:N} = \mathbf{0}, \Theta)$ in (13). However, the naive method fails to converge to the true posteriors. In contrast, the DALTON posteriors are almost indistinguishable from the true posteriors at $\Delta t = 0.1$, corroborating our heuristic justification of convergence in Section 3.3.

5.3 Lorenz63 Model

The Lorenz63 model [31] relates the properties of a fluid layer induced by a warm temperature above and a cool temperature below. Lorenz63 is a system of three ordinary differential equations on $\mathbf{x}(t) = (x(t), y(t), z(t))$ known as the Lorenz equations, which are given by

$$\frac{dx(t)}{dt} = \alpha(y(t) - x(t)), \quad \frac{dy(t)}{dt} = x(t)(\rho - z(t)) - y(t), \quad \frac{dz(t)}{dt} = x(t)y(t) - \beta z(t). \quad (24)$$

It contains six parameters $\theta = (\alpha, \rho, \beta, x(0), y(0), z(0))$, with $\alpha, \rho, \beta > 0$. The measurement error model is

$$\mathbf{Y}_i \stackrel{\text{ind}}{\sim} \mathcal{N}(\mathbf{x}(t_i), \phi^2 \cdot \mathbf{I}_{2 \times 2}), \quad (25)$$

where $t_i = i$ with $i = 0, 1, \dots, 20$ and $\phi^2 = 0.005$.

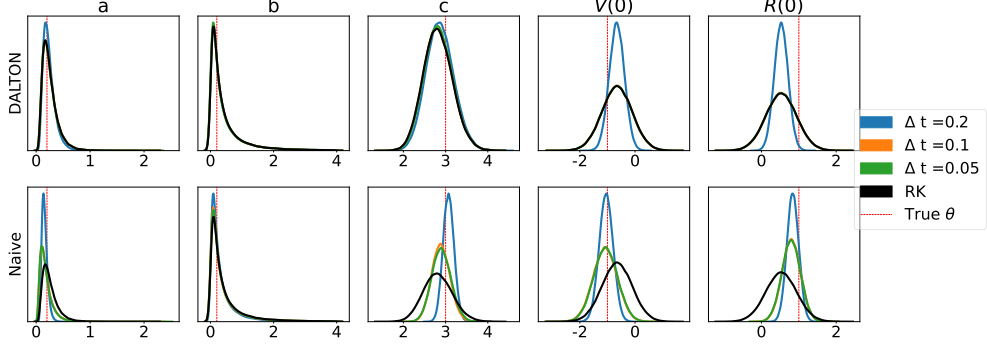


Figure 2: Parameter posteriors for the FN model for the non-Gaussian DALTON and its naive Gaussian approximation.

Before conducting parameter inference, we first estimate the ODE with the Fenrir and DALTON solvers and compare them to true ODE produced by RK. The corresponding curves are displayed in Figure 3, with true parameter value $\theta = (28, 10, 8/3, -12, -5, 38)$ and DALTON and Fenrir step size $\Delta t = 0.005$. Fenrir struggles with the chaotic nature of the Lorenz63 model, being able to incorporate information from the data only on the backward pass. In contrast, DALTON effectively uses the observations on the forward pass to produce a solution close to the ground truth.

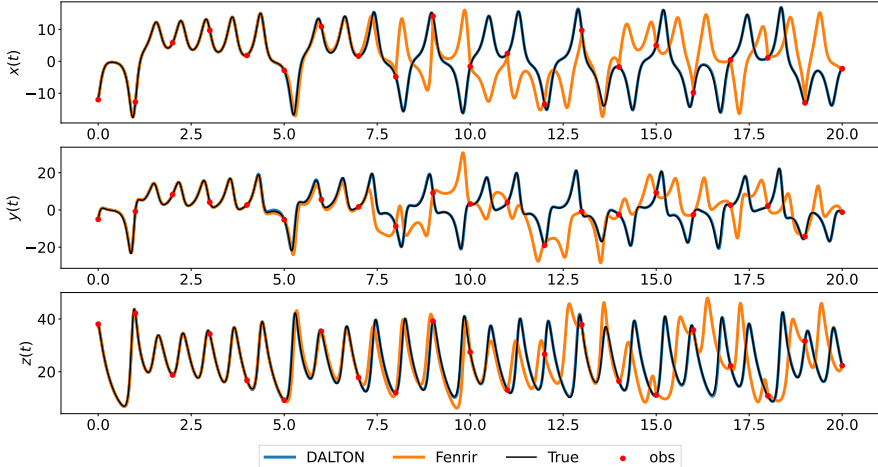


Figure 3: ODE for the Lorenz63 model calculated using various solvers.

Figure 4 displays the Laplace posteriors for the DALTON, Fenrir, and RK methods. The DALTON posteriors all cover the true parameter values. Both Fenrir and RK posteriors do so as well, but with vanishingly little uncertainty. However, this appears to be because the optimization algorithms, initialized at the true parameter values, were not able to escape the deep local optima of the Fenrir and RK likelihoods.

In order to investigate this claim, we modify the parameter learning problem so that $t_i = i/10$ with $i = 0, 1, \dots, 200$ and with parameters $x(0)$, $y(0)$, and $z(0)$ are assumed to be known. Figure 5 displays optimized parameters α , ρ , and β against several different starting values for DALTON, Fenrir and RK. When initialized far from the ground truth, Fenrir and RK fail to converge to the correct parameter values. Since the posterior uncertainty in all cases is negligible, even the true Laplace posterior produced by RK is unusable for parameter inference. In contrast, DALTON is able

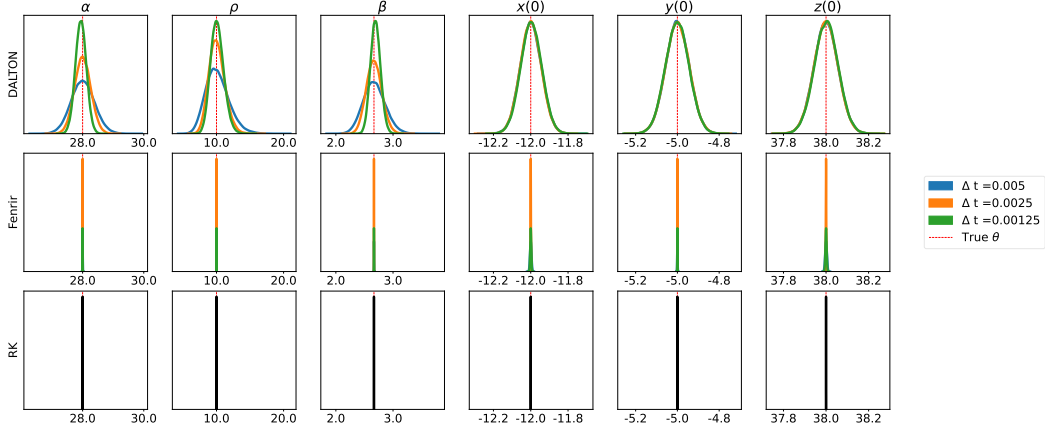


Figure 4: Parameter posteriors for the Lorenz63 model using various ODE solvers.

to converge to the true parameters at a wide range of initial values, and retains the parameter coverage exhibited in Figure 4.

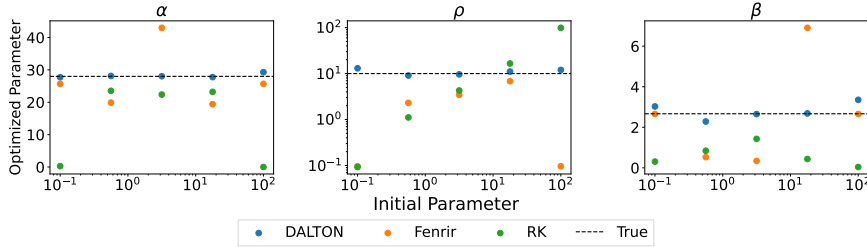


Figure 5: Initial and optimized parameter values for the Lorenz63 model using various ODE solvers.

6 Conclusion

We present DALTON, a probabilistic approximation to the intractable likelihood of ODE-IVP problems. By incorporating information from the observed data in an online manner, DALTON can greatly reduce the sensitivity of many ODE systems to parameter values, thus providing more reliable parameter estimates than many other probabilistic ODE solvers, and in cases of extreme parameter hypersensitivity, than the exact ODE likelihood itself. DALTON achieves this in a computationally competitive linear scaling regime by building on a well-established paradigm of Bayesian filtering which makes heavy use of the Kalman filtering and smoothing recursions. One limitation of the DALTON solver is the determination the appropriate step size, which could be done adaptively as described in [38]. There is also potential to explore the effectiveness of DALTON in estimating the parameters of stiff ODE systems, and to extend it to more complex boundary conditions.

References

- [1] K. Atkinson, W. Han, and D. E. Stewart. *Numerical Solution of Ordinary Differential Equations*. John Wiley & Sons, 2009. ISBN 978-0-470-04294-6.
- [2] D. Barber and Y. Wang. Gaussian processes for Bayesian estimation in ordinary differential equations. In E. P. Xing and T. Jebara, editors, *Proceedings of the 31st international conference on machine learning*, volume 32 of *Proceedings of machine learning research*, pages 1485–1493, Bejing, China, 2014. PMLR. URL <https://proceedings.mlr.press/v32/barber14.html>.

[3] M. Blondel, Q. Berthet, M. Cuturi, R. Frostig, S. Hoyer, F. Llinares-López, F. Pedregosa, and J.-P. Vert. Efficient and modular implicit differentiation. *arXiv preprint arXiv:2105.15183*, 2021.

[4] N. Bosch, P. Hennig, and F. Tronarp. Calibrated adaptive probabilistic ODE solvers. In A. Banerjee and K. Fukumizu, editors, *Proceedings of The 24th International Conference on Artificial Intelligence and Statistics*, volume 130 of *Proceedings of Machine Learning Research*, pages 3466–3474. PMLR, 13–15 Apr 2021. URL <https://proceedings.mlr.press/v130/bosch21a.html>.

[5] N. Bosch, F. Tronarp, and P. Hennig. Pick-and-mix information operators for probabilistic ODE solvers. In G. Camps-Valls, F. J. R. Ruiz, and I. Valera, editors, *Proceedings of The 25th International Conference on Artificial Intelligence and Statistics*, volume 151 of *Proceedings of Machine Learning Research*, pages 10015–10027. PMLR, 28–30 Mar 2022. URL <https://proceedings.mlr.press/v151/bosch22a.html>.

[6] J. Bradbury, R. Frostig, P. Hawkins, M. J. Johnson, C. Leary, D. Maclaurin, G. Necula, A. Paszke, J. VanderPlas, S. Wanderman-Milne, and Q. Zhang. JAX: composable transformations of Python+NumPy programs, 2018. URL <http://github.com/google/jax>.

[7] J. C. Butcher. *Numerical Methods for Ordinary Differential Equations*. John Wiley & Sons, 2008.

[8] B. Calderhead, M. Girolami, and N. D. Lawrence. Accelerating Bayesian inference over nonlinear differential equations with Gaussian processes. In *Advances in neural information processing systems*, pages 217–224, 2009.

[9] J. Cao, L. Wang, and J. Xu. Robust estimation for ordinary differential equation models. *Biometrics*, 67(4):1305–1313, 2011. doi: <https://doi.org/10.1111/j.1541-0420.2011.01577.x>. URL <https://onlinelibrary.wiley.com/doi/abs/10.1111/j.1541-0420.2011.01577.x>.

[10] O. A. Chkrebtii, D. A. Campbell, B. Calderhead, and M. A. Girolami. Bayesian solution uncertainty quantification for differential equations. *Bayesian Analysis*, 11(4):1239–1267, December 2016. ISSN 1936-0975. doi: 10.1214/16-BA1017. URL <https://projecteuclid.org/euclid.ba/1473276259>.

[11] P. R. Conrad, M. Girolami, S. Särkkä, A. Stuart, and K. Zygalakis. Statistical analysis of differential equations: introducing probability measures on numerical solutions. *Statistics and Computing*, 27(4):1065–1082, July 2017. ISSN 0960-3174, 1573-1375. doi: 10.1007/s11222-016-9671-0. URL <http://link.springer.com/10.1007/s11222-016-9671-0>.

[12] S. Dass, J. Lee, K. Lee, and J. Park. Laplace based approximate posterior inference for differential equation models. *Statistics and Computing*, 27(3):679–698, may 2017. ISSN 0960-3174. doi: 10.1007/s11222-016-9647-0.

[13] P. Diaconis. Bayesian numerical analysis. In J. Berger and S. Gupta, editors, *Statistical Decision Theory and Related Topics IV*, volume 1, pages 163–175. Springer-Verlag, New York, 1988.

[14] F. Dondelinger, D. Husmeier, S. Rogers, and M. Filippone. ODE parameter inference using adaptive gradient matching with Gaussian processes. In C. M. Carvalho and P. Ravikumar, editors, *Proceedings of the sixteenth international conference on artificial intelligence and statistics*, volume 31 of *Proceedings of machine learning research*, pages 216–228, Scottsdale, Arizona, USA, 2013. PMLR. URL <https://proceedings.mlr.press/v31/dondelinger13a.html>.

[15] J. R. Dormand and P. J. Prince. A family of embedded Runge-Kutta formulae. *Journal of Computational and Applied Mathematics*, 6(1):19–26, 1980. Publisher: Elsevier.

[16] W. Frank, T. Stefan, S. Dirk, L. Uwe, and W. Claus. Sensitivity analysis of ordinary differential equation models. Technical report, Technische Universität Dortmund, 2018.

[17] A. Gelman, J. B. Carlin, H. S. Stern, D. B. Dunson, A. Vehtari, and D. B. Rubin. *Bayesian Data Analysis*. Chapman & Hall, New York, NY, 3rd edition, 2013. ISBN 978-0-429-11307-9.

[18] S. Ghosh, S. Dasmahapatra, and K. Maharatna. Fast approximate Bayesian computation for estimating parameters in differential equations. *Statistics and Computing*, 27(1):19–38, 2017. ISSN 0960-3174, 1573-1375. doi: 10.1007/s11222-016-9643-4. URL <http://link.springer.com/10.1007/s11222-016-9643-4>.

[19] N. Gianniotis. Mixed variational inference. In *2019 International Joint Conference on Neural Networks (IJCNN)*, pages 1–8, Budapest, Hungary, 2019. IEEE. ISBN 978-1-72811-985-4. doi: 10.1109/IJCNN.2019.8852348. URL <https://ieeexplore.ieee.org/document/8852348/>.

[20] N. S. Gorbach, S. Bauer, and J. M. Buhmann. Scalable variational inference for dynamical systems. In *Proceedings of the 31st international conference on neural information processing systems*, NIPS’17, pages 4809–4818, Red Hook, NY, USA, 2017. Curran Associates Inc. ISBN 978-1-5108-6096-4.

[21] D. F. Griffiths and D. J. Higham. *Numerical Methods for Ordinary Differential Equations: Initial Value Problems*. Springer Science & Business Media, 2010.

[22] P. Hennig, M. A. Osborne, and M. Girolami. Probabilistic numerics and uncertainty in computations. *Proceedings of the Royal Society A: Mathematical, Physical and Engineering Sciences*, 471(2179):20150142, July 2015. ISSN 1364-5021, 1471-2946. doi: 10.1098/rspa.2015.0142. URL <https://royalsocietypublishing.org/doi/10.1098/rspa.2015.0142>.

[23] H. Kersting and P. Hennig. Active uncertainty calibration in Bayesian ODE solvers. In *32nd conference on uncertainty in artificial intelligence (UAI 2016)*, pages 309–318, 2016.

[24] H. Kersting, N. Krämer, M. Schiegg, C. Daniel, M. Tiemann, and P. Hennig. Differentiable likelihoods for fast inversion of likelihood-free dynamical systems. In H. D. III and A. Singh, editors, *Proceedings of the 37th International Conference on Machine Learning*, volume 119 of *Proceedings of Machine Learning Research*, pages 5198–5208. PMLR, 13–18 Jul 2020. URL <https://proceedings.mlr.press/v119/kersting20a.html>.

[25] H. Kersting, T. Sullivan, and P. Hennig. Convergence rates of Gaussian ODE filters. *Statistics and Computing*, 30:1–26, 11 2020. doi: 10.1007/s11222-020-09972-4.

[26] P. Kidger. *On Neural Differential Equations*. PhD thesis, University of Oxford, 2021. URL <https://arxiv.org/pdf/2202.02435.pdf>.

[27] R. C. Kohberger, D. Scavia, and J. W. Wilkinson. A method for parameter sensitivity analysis in differential equation models. *Water Resources Research*, 14(1):25–29, 1978. doi: <https://doi.org/10.1029/WR014i001p00025>. URL <https://agupubs.onlinelibrary.wiley.com/doi/abs/10.1029/WR014i001p00025>.

[28] N. Krämer and P. Hennig. Stable implementation of probabilistic ODE solvers. 2020. doi: 10.48550/ARXIV.2012.10106. URL <https://arxiv.org/abs/2012.10106>.

[29] N. Krämer, N. Bosch, J. Schmidt, and P. Hennig. Probabilistic ODE solutions in millions of dimensions. 10 2021. URL <https://proceedings.mlr.press/v162/kramer22b/kramer22b.pdf>.

[30] A. Lazarus, D. Husmeier, and T. Papamarkou. Multiphase MCMC sampling for parameter inference in nonlinear ordinary differential equations. In A. Storkey and F. Perez-Cruz, editors, *Proceedings of the twenty-first international conference on artificial intelligence and statistics*, volume 84 of *Proceedings of machine learning research*, pages 1252–1260. PMLR, 2018. URL <https://proceedings.mlr.press/v84/lazarus18a.html>.

[31] E. N. Lorenz. Deterministic nonperiodic flow. *Journal of Atmospheric Sciences*, 20:130–141, 1963. ISSN 1520-0469. URL <https://journals.ametsoc.org/doi/pdf/10.1175/1520-0469%281963%29020%3C0130%3ADNF%3E2.0.CO%3B2>.

[32] D. J. C. MacKay. A practical Bayesian framework for backpropagation networks. *Neural Computation*, 4(3):448–472, 1992. ISSN 0899-7667, 1530-888X. doi: 10.1162/neco.1992.4.3.448. URL <https://direct.mit.edu/neco/article/4/3/448-472/5654>.

[33] J. Nocedal and S. J. Wright. *Numerical Optimization*. Springer, New York, NY, USA, 2e edition, 2006.

[34] C. Rackauckas, Y. Ma, V. Dixit, X. Guo, M. Innes, J. Revels, J. Nyberg, and V. Ivaturi. A comparison of automatic differentiation and continuous sensitivity analysis for derivatives of differential equation solutions. *CoRR*, abs/1812.01892, 2018. URL <http://arxiv.org/abs/1812.01892>.

[35] C. Rocsoreanu, A. Georgescu, and N. Giurgiteanu. *The FitzHugh-Nagumo model: Bifurcation and Dynamics*, volume 10. Springer Science & Business Media, 2012.

[36] J. Schmidt, N. Krämer, and P. Hennig. A probabilistic state space model for joint inference from differential equations and data. In M. Ranzato, A. Beygelzimer, Y. Dauphin, P. Liang, and J. W. Vaughan, editors, *Advances in Neural Information Processing Systems*, volume 34, pages 12374–12385. Curran Associates, Inc., 2021. URL https://proceedings.neurips.cc/paper_files/paper/2021/file/6734fa703f6633ab896eecd9fad8953a-Paper.pdf.

[37] M. Schober, D. K. Duvenaud, and P. Hennig. Probabilistic ODE solvers with Runge-Kutta means. In *Advances in neural information processing systems*, pages 739–747, 2014.

[38] M. Schober, S. Särkkä, and P. Hennig. A probabilistic model for the numerical solution of initial value problems. *Statistics and Computing*, 29(1):99–122, January 2019. ISSN 0960-3174, 1573-1375. doi: 10.1007/s11222-017-9798-7. URL <http://link.springer.com/10.1007/s11222-017-9798-7>.

[39] W. E. Sherwood. *FitzHugh–Nagumo Model*, pages 1–11. Springer New York, New York, NY, 2013. ISBN 978-1-4614-7320-6. doi: 10.1007/978-1-4614-7320-6_147-1. URL https://doi.org/10.1007/978-1-4614-7320-6_147-1.

[40] J. Skilling. Bayesian solution of ordinary differential equations. In C. R. Smith, G. J. Erickson, and P. O. Neudorfer, editors, *Maximum Entropy and Bayesian Methods: Seattle, 1991*, Fundamental Theories of Physics, pages 23–37. Springer Netherlands, Dordrecht, 1992. ISBN 978-94-017-2219-3. doi: 10.1007/978-94-017-2219-3_2. URL https://doi.org/10.1007/978-94-017-2219-3_2.

[41] O. Teymur, K. Zygalakis, and B. Calderhead. Probabilistic linear multistep methods. In *Advances in Neural Information Processing Systems 29*, pages 4321–4328. Curran Associates, Inc., 2016.

[42] F. Tronarp, H. Kersting, S. Särkkä, and P. Hennig. Probabilistic solutions to ordinary differential equations as non-linear Bayesian filtering: a new perspective. *arXiv:1810.03440 [stat]*, October 2018. URL <http://arxiv.org/abs/1810.03440>. arXiv: 1810.03440.

[43] F. Tronarp, N. Bosch, and P. Hennig. Fenrir: Physics-enhanced regression for initial value problems. In K. Chaudhuri, S. Jegelka, L. Song, C. Szepesvari, G. Niu, and S. Sabato, editors, *Proceedings of the 39th International Conference on Machine Learning*, volume 162 of *Proceedings of Machine Learning Research*, pages 21776–21794. PMLR, 17–23 Jul 2022. URL <https://proceedings.mlr.press/v162/tronarp22a.html>.

[44] J. Wenger, N. Krämer, M. Pförtner, J. Schmidt, N. Bosch, N. Effenberger, J. Zenn, A. Gessner, T. Karvonen, F.-X. Briol, M. Mahsereci, and P. Hennig. Probnum: Probabilistic numerics in Python, 2021. URL <https://arxiv.org/abs/2112.02100>.

[45] P. Wenk, A. Gotovos, S. Bauer, N. S. Gorbach, A. Krause, and J. M. Buhmann. Fast Gaussian process based gradient matching for parameter identification in systems of nonlinear ODEs. In K. Chaudhuri and M. Sugiyama, editors, *Proceedings of the twenty-second international conference on artificial intelligence and statistics*, volume 89 of *Proceedings of machine learning research*, pages 1351–1360. PMLR, 2019. URL <https://proceedings.mlr.press/v89/wenk19a.html>.

[46] S. Yang, S. W. K. Wong, and S. C. Kou. Inference of dynamic systems from noisy and sparse data via manifold-constrained Gaussian processes. *Proceedings of the National Academy of Sciences*, 118(15):e2020397118, 2021. ISSN 0027-8424, 1091-6490. doi: 10.1073/pnas.2020397118. URL <http://www.pnas.org/lookup/doi/10.1073/pnas.2020397118>.

A Gaussian Markov Process Prior

Recall from (1) that for a multi-variable function $\mathbf{x}(t) = (x_1(t), \dots, x_d(t))$, we define $\mathbf{X}(t) = (\mathbf{X}_1(t), \dots, \mathbf{X}_d(t))$ with $\mathbf{X}_k(t) = (x_k^{(0)}(t), \dots, x_k^{(q_k-1)}(t))$ containing the first $q_k - 1$ derivatives of $x_k(t) = x_k^{(0)}(t)$. Similarly, we define the initial value to be $\mathbf{v} = (v_1, \dots, v_d)$, and the coefficient matrix to be $\mathbf{W} = (\mathbf{W}_1, \dots, \mathbf{W}_d)$. DALTON uses a simple and effective prior proposed by [38]; namely, that each $\mathbf{X}_k(t)$, $k = 1, \dots, d$ are independent $p - 1$ times integrated Brownian motion (IBM),

$$\tilde{x}_k^{(p-1)}(t) = \sigma_k B_k(t), \quad (26)$$

where $p = \max q_k + 1$. Here we choose $p = \max q_k + 1$ because it is often advantageous in practice to set $p > q_k$ to increase the smoothness of $\mathbf{X}_k(t)$ and at the same time keep p small to reduce complexity. This results in a p -dimensional continuous Gaussian Markov process on $\mathbf{X}_k(t)$ defined by

$$\mathbf{X}_k(t + \Delta t) \mid \mathbf{X}_k(t) \sim \mathcal{N}(\mathbf{Q}^{(k)} \mathbf{X}_k(t), \mathbf{R}^{(k)}), \quad (27)$$

with matrices $\mathbf{Q}^{(k)}$ and $\mathbf{R}^{(k)}$ given by

$$Q_{ij}^{(k)} = \mathbb{1}_{i \leq j} \frac{(\Delta t)^{j-i}}{(j-1)!}, \quad R_{ij}^{(k)} = \sigma_k^2 \frac{(\Delta t)^{2p+1-i-j}}{(2p+1-i-j)(p-i)!(p-j)!}. \quad (28)$$

The corresponding matrices in (3) are $\mathbf{Q} = \text{diag}(\mathbf{Q}_{p \times p}^{(1)}, \dots, \mathbf{Q}_{p \times p}^{(d)})$ and $\mathbf{R} = \text{diag}(\mathbf{R}_{p \times p}^{(1)}, \dots, \mathbf{R}_{p \times p}^{(d)})$. Furthermore, for each $k = 1, \dots, d$ we pad \mathbf{v}_k and \mathbf{W}_k in (1) with $p - q_k$ zeros and $p_k - q_k$ columns of zeros, respectively, to guarantee \mathbf{W} to be block diagonal. A different method of padding \mathbf{v}_k is to work out the values of $x^{(l)}(0)$ for $q_k \leq l < p$ by taking derivatives of the ODE in (1).

B Kalman Functions

The formulations for the Kalman functions used in Algorithms 1 and 2 are as follows.

Algorithm 3 Standard Kalman filtering and smoothing functions.

```

▷ Perform the prediction step.
1: procedure KALMAN_PREDICT( $\mu_{n-1|n-1}$ ,  $\Sigma_{n-1|n-1}$ ,  $\mathbf{c}$ ,  $\mathbf{Q}$ ,  $\mathbf{R}$ )
2:    $\mu_{n|n-1} \leftarrow \mathbf{Q}\mu_{n-1|n-1} + \mathbf{c}$ 
3:    $\Sigma_{n|n-1} \leftarrow \mathbf{Q}\Sigma_{n-1|n-1}\mathbf{Q}' + \mathbf{R}$ 
4:   return  $\mu_{n|n-1}$ ,  $\Sigma_{n|n-1}$  ▷ Predicted mean and variance:  $E[\mathbf{X}_n | \mathbf{Z}_{0:n-1}]$ ,  $\text{var}[\mathbf{X}_n | \mathbf{Z}_{0:n-1}]$ 

▷ Perform the update step.
5: procedure KALMAN_UPDATE( $\mu_{n|n-1}$ ,  $\Sigma_{n|n-1}$ ,  $\mathbf{W}$ ,  $\mathbf{z}_n$ ,  $\mathbf{a}_n$ ,  $\mathbf{B}_n$ ,  $\mathbf{V}_n$ )
6:    $\tilde{\mathbf{W}}_n \leftarrow \mathbf{W} + \mathbf{B}_n$ 
7:    $\mathbf{A}_n \leftarrow \Sigma_{n|n-1}\tilde{\mathbf{W}}_n'[\tilde{\mathbf{W}}_n\Sigma_{n|n-1}\tilde{\mathbf{W}}_n' + \mathbf{V}_n]^{-1}$ 
8:    $\mu_{n|n} \leftarrow \mu_{n|n-1} + \mathbf{A}_n(\mathbf{z}_n - \tilde{\mathbf{W}}_n\mu_{n|n-1} - \mathbf{a}_n)$ 
9:    $\Sigma_{n|n} \leftarrow \Sigma_{n|n-1} - \mathbf{A}_n\tilde{\mathbf{W}}_n\Sigma_{n|n-1}$ 
10:  return  $\mu_{n|n}$ ,  $\Sigma_{n|n}$  ▷ Updated mean and variance:  $E[\mathbf{X}_n | \mathbf{Z}_{0:n}]$ ,  $\text{var}[\mathbf{X}_n | \mathbf{Z}_{0:n}]$ 

▷ Perform the forecast step.
11: procedure KALMAN_FORECAST( $\mu_{n|n-1}$ ,  $\Sigma_{n|n-1}$ ,  $\mathbf{a}_n$ ,  $\mathbf{B}_n\mathbf{V}_n$ )
12:    $\mu_n \leftarrow \mathbf{B}_n\mu_{n|n-1} + \mathbf{a}_n$ 
13:    $\Sigma_n \leftarrow \mathbf{B}_n\mu_{n|n-1}\mathbf{B}_n' + \mathbf{V}_n$ 
14:   return  $\mu_n$ ,  $\Sigma_n$  ▷ Forecasted mean and variance:  $E[\mathbf{Z}_n | \mathbf{Z}_{0:n-1}]$ ,  $\text{var}[\mathbf{Z}_n | \mathbf{Z}_{0:n-1}]$ 

▷ Perform the sampler smoothing step.
15: procedure KALMAN_SAMPLE( $\mathbf{x}_{n+1}$ ,  $\mu_{n|n}$ ,  $\Sigma_{n|n}$ ,  $\mu_{n+1|n}$ ,  $\Sigma_{n+1|n}$ ,  $\mathbf{Q}$ )
16:    $\mathbf{A}_n \leftarrow \Sigma_{n|n}\mathbf{Q}'\Sigma_{n+1|n}^{-1}$ 
17:    $\tilde{\mu}_{n|N} \leftarrow \mu_{n|n} + \mathbf{A}_n(\mathbf{x}_{n+1} - \mu_{n+1|n})$ 
18:    $\tilde{\Sigma}_{n|N} \leftarrow \Sigma_{n|n} - \mathbf{A}_n\mathbf{Q}\Sigma_{n|n}$ 
19:   return  $\tilde{\mu}_{n|N}$ ,  $\tilde{\Sigma}_{n|N}$  ▷ Smoothing sampler mean and variance:
    $E[\mathbf{X}_n | \mathbf{X}_{n+1}, \mathbf{Z}_{0:N}]$ ,  $\text{var}[\mathbf{X}_n | \mathbf{X}_{n+1}, \mathbf{Z}_{0:N}]$ 

▷ Perform the smoothing step.
20: procedure KALMAN_SMOOTH( $\mu_{n+1|N}$ ,  $\Sigma_{n+1|N}$ ,  $\mu_{n|n}$ ,  $\Sigma_{n|n}$ ,  $\mu_{n+1|n}$ ,  $\Sigma_{n+1|n}$ ,  $\mathbf{Q}$ )
21:    $\mathbf{A}_n \leftarrow \Sigma_{n|n}\mathbf{Q}'\Sigma_{n+1|n}^{-1}$ 
22:    $\mu_{n|N} \leftarrow \mu_{n|n} + \mathbf{A}_n(\mu_{n+1|N} - \mu_{n+1|n})$ 
23:    $\Sigma_{n|N} \leftarrow \Sigma_{n|n} + \mathbf{A}_n(\Sigma_{n+1|N} - \Sigma_{n+1|n})\mathbf{A}_n$ 
24:   return  $\mu_{n|N}$ ,  $\Sigma_{n|N}$  ▷ Smoothing mean and variance:  $E[\mathbf{X}_n | \mathbf{Z}_{0:N}]$ ,  $\text{var}[\mathbf{X}_n | \mathbf{Z}_{0:N}]$ 

```

C DALTON Algorithm for Non-Gaussian Measurements

Algorithm 2 DALTON probabilistic ODE likelihood approximation for non-Gaussian measurements.

```

1: procedure DALTONNG( $\mathbf{W}_\theta, \mathbf{f}(\mathbf{X}, t, \theta), \mathbf{v}_\theta, \mathbf{Q}_\eta, \mathbf{R}_\eta, \mathbf{Y}_{0:M}, \phi, \mathbf{g}_{0:M}(\mathbf{x}, \mathbf{Y}, \phi)$ )
2:    $\mu_{0|0}, \Sigma_{0|0} \leftarrow \mathbf{v}, \mathbf{0}$                                  $\triangleright$  Initialization
3:    $\mathbf{Z}_{0:N} \leftarrow \mathbf{0}$ 
4:    $\ell_{xz}, \ell_{xyz}, \ell_y \leftarrow 0, 0, 0$ 
5:    $i \leftarrow 0$                                           $\triangleright$  Used to map  $t_n$  to  $t'_i$ 
6:    $\triangleright$  Lines 7-24 compute  $\log p(\mathbf{X}_{0:N} \mid \hat{\mathbf{Y}}_{0:M}, \mathbf{Z}_{0:N} = \mathbf{0}, \Theta)$ 
7:   for  $n = 1 : N$  do
8:      $\mu_{n|n-1}, \Sigma_{n|n-1} \leftarrow \text{kalman\_predict}(\mu_{n-1|n-1}, \Sigma_{n-1|n-1}, \mathbf{0}, \mathbf{Q}_\eta, \mathbf{R}_\eta)$ 
9:      $\mathbf{a}_n, \mathbf{B}_n, \mathbf{V}_n \leftarrow \text{linearize}(\mu_{n|n-1}, \Sigma_{n|n-1}, \mathbf{W}_\theta, \mathbf{f}(\mathbf{X}, t_n, \phi))$ 
10:    if  $t_n = t_{n(i)}$  then
11:       $\hat{\mathbf{x}}_n \leftarrow \text{subset}(\mu_{n-1|n-1}, t_n)$ 
12:       $g \leftarrow g_i(\hat{\mathbf{x}}_n, \mathbf{Y}_i, \phi)$ 
13:       $\mathbf{g}_{(1)} \leftarrow \nabla g_i(\hat{\mathbf{x}}_n, \mathbf{Y}_i, \phi)$ 
14:       $\mathbf{g}_{(2)} \leftarrow \nabla^2 g_i(\hat{\mathbf{x}}_n, \mathbf{Y}_i, \phi)$ 
15:       $\hat{\mathbf{Y}}_i \leftarrow \hat{\mathbf{x}}_n - \mathbf{g}_{(2)}^{-1} \mathbf{g}_{(1)}$   $\triangleright$  Compute pseudo-observations
16:       $\mathbf{Z}_n \leftarrow \begin{bmatrix} \mathbf{Z}_n \\ \hat{\mathbf{Y}}_i \end{bmatrix}, \quad \mathbf{W}_\theta \leftarrow \begin{bmatrix} \mathbf{W}_\theta \\ \mathbf{D}_i \end{bmatrix}, \quad \mathbf{B}_n \leftarrow \begin{bmatrix} \mathbf{B}_n \\ \mathbf{0} \end{bmatrix}$ 
17:       $\mathbf{a}_n \leftarrow \begin{bmatrix} \mathbf{a}_n \\ \mathbf{0} \end{bmatrix}, \quad \mathbf{V}_n \leftarrow \begin{bmatrix} \mathbf{V}_n & \mathbf{0} \\ \mathbf{0} & g''^{-1} \end{bmatrix}$ 
18:       $i \leftarrow i + 1$ 
19:     $\mu_{n|n}, \Sigma_{n|n} \leftarrow \text{kalman\_update}(\mu_{n|n-1}, \Sigma_{n|n-1}, \mathbf{W}_\theta, \mathbf{Z}_n, \mathbf{a}_n, \mathbf{B}_n, \mathbf{V}_n)$ 
20:   for  $n = N - 1 : 1$  do
21:      $\mu_{n|N}, \Sigma_{n|N} \leftarrow \text{kalman\_smooth}(\mu_{n+1|N}, \Sigma_{n+1|N}, \mu_{n|n}, \Sigma_{n|n}, \mu_{n+1|n}, \Sigma_{n+1|n}, \mathbf{Q}_\eta)$ 
22:      $\mu_n, \Sigma_n \leftarrow \text{kalman\_sample}(\mu_{n+1|N}, \mu_{n|n}, \Sigma_{n|n}, \mu_{n+1|n}, \Sigma_{n+1|n}, \mathbf{Q}_\eta)$ 
23:      $\ell_{xyz} \leftarrow \ell_{xyz} + \text{normal\_logpdf}(\mu_{n|N}; \mu_n, \Sigma_n)$ 
24:      $\ell_{xyz} \leftarrow \ell_{xyz} + \text{normal\_logpdf}(\mu_{N|N}; \mu_{N|N}, \Sigma_{N|N})$ 
25:      $\triangleright$  Lines 26-35 compute  $\log p(\mathbf{X}_{0:N} \mid \mathbf{Z}_{0:N} = \mathbf{0}, \Theta)$ 
26:      $\mathbf{Z}_{0:N} \leftarrow \mathbf{0}$   $\triangleright$  Reset  $\mathbf{Z}_{0:N} = \mathbf{0}$ 
27:      $\mu'_{0:N|N} \leftarrow \mu_{0:N|N}$   $\triangleright$  Store  $\mu_{0:N|N} = E[\mathbf{X}_{0:N} \mid \mathbf{Z}_{0:N}, \hat{\mathbf{Y}}_{0:N}]$  for later
28:   for  $n = 1 : N$  do
29:      $\mu_{n|n-1}, \Sigma_{n|n-1} \leftarrow \text{kalman\_predict}(\mu_{n-1|n-1}, \Sigma_{n-1|n-1}, \mathbf{0}, \mathbf{Q}_\eta, \mathbf{R}_\eta)$ 
30:      $\mathbf{a}_n, \mathbf{B}_n, \mathbf{V}_n \leftarrow \text{linearize}(\mu_{n|n-1}, \Sigma_{n|n-1}, \mathbf{W}_\theta, \mathbf{f}(\mathbf{X}, t_n, \phi))$ 
31:      $\mu_{n|n}, \Sigma_{n|n} \leftarrow \text{kalman\_update}(\mu_{n|n-1}, \Sigma_{n|n-1}, \mathbf{W}_\theta, \mathbf{Z}_n, \mathbf{a}_n, \mathbf{B}_n, \mathbf{V}_n)$ 
32:   for  $n = N - 1 : 1$  do
33:      $\mu_n, \Sigma_n \leftarrow \text{kalman\_sample}(\mu'_{n+1|N}, \mu_{n|n}, \Sigma_{n|n}, \mu_{n+1|n}, \Sigma_{n+1|n}, \mathbf{Q}_\eta)$ 
34:      $\ell_{xz} \leftarrow \ell_{xz} + \text{normal\_logpdf}(\mu'_{n|N}; \mu_n, \Sigma_n)$ 
35:      $\ell_{xz} \leftarrow \ell_{xz} + \text{normal\_logpdf}(\mu'_{N|N}; \mu_{N|N}, \Sigma_{N|N})$ 
36:      $\triangleright$  Lines 37-39 compute  $\log p(\mathbf{Y}_{0:M} \mid \mathbf{X}_{0:N}, \phi)$ 
37:   for  $i = 0 : M$  do
38:      $\mathbf{x}_i \leftarrow \text{subset}(\mu'_{n(i)|N}, t_{n(i)})$ 
39:      $\ell_y \leftarrow \ell_y + g_i(\mathbf{Y}_i; \mathbf{x}_i, \phi)$ 
40:
41:   return  $\ell_{xz} - \ell_y - \ell_{xyz}$   $\triangleright$  Estimate of  $\log p(\mathbf{Y}_{0:M} \mid \mathbf{Z}_{0:N} = \mathbf{0}, \Theta)$ 

```

D First-Order Taylor Linearization

The first order Taylor approximation of $\mathbf{f}(\mathbf{X}_n, t_n)$ in (2) proposed by Tronarp et al. [42] also known as the extended Kalman filter (EKF) is

$$\mathbf{f}(\mathbf{X}_n, t_n) \approx \mathbf{f}(\boldsymbol{\mu}_{n|n-1}) + J_f(\boldsymbol{\mu}_{n|n-1})(\mathbf{X}_n - \boldsymbol{\mu}_{n|n-1}) \quad (29)$$

where $\boldsymbol{\mu}_{n|n-1} = E[\mathbf{X}_n | \mathbf{Z}_{1:n-1}]$, and J_f is the Jacobian of $\mathbf{X} \rightarrow \mathbf{f}(\mathbf{X}, t)$.

For a multivariate ODE, a substantial computation speedup from $\mathcal{O}(\{\sum_{k=1}^d q_k\}^3)$ to $\mathcal{O}(\prod_{k=1}^d q_k^3)$ in the Kalman filter is to assume each matrix in (3) is block diagonal [29]. This can be done by assuming the priors for each variable is independent, such that, the prior matrices, \mathbf{Q} and \mathbf{R} , and the coefficient matrix, \mathbf{W} , are block diagonal [29]. The only remaining matrices in (3) are \mathbf{B}_n and \mathbf{V}_n . For the zeroth order Taylor approximation, both $\mathbf{B}_n = \mathbf{V}_n = \mathbf{0}$. In the first order case, the Jacobian, J_f , is not necessarily block diagonal. However, it is noted that keeping only the block diagonal elements of J_f only slightly reduces numerical accuracy [29]. Denoting the block diagonal of J_f as $\text{bd}(J_f)$, and setting $\mathbf{a}_n = -\mathbf{f}(\boldsymbol{\mu}_{n|n-1}) + \text{bd}(J_f)(\boldsymbol{\mu}_{n|n-1})\boldsymbol{\mu}_{n|n-1}$, $\mathbf{B}_n = -\text{bd}(J_f)(\boldsymbol{\mu}_{n|n-1})$ and $\mathbf{V}_n = 0$ ensures all matrices in (3) are block diagonal.